Bayesian Graph Traversal

William N. Caballero^a, Phillip R. Jenkins^a, David Banks^b, Matthew Robbins^a

^aDepartment of Operational Sciences, Air Force Institute of Technology, WPAFB, OH ^bDepartment of Statistical Science, Duke University, Durham, NC

Abstract

This research considers Bayesian decision-analytic approaches toward the traversal of an uncertain graph. Namely, a traveler progresses over a graph in which rewards are gained upon a node's first visit and costs are incurred for every edge traversal. The traveler knows the graph's adjacency matrix and his starting position, but does not know the rewards and costs. The traveler is a Bayesian who encodes his beliefs about these values using a Gaussian process prior and who seeks to maximize his expected utility over these beliefs. Adopting a decision-analytic perspective, we develop sequential decision-making solution strategies for this coupled information-collection and network-routing problem. We show that the problem is NP-Hard, and derive properties of the optimal walk. These properties provide heuristics for the traveler's problem that balance exploration and exploitation. We provide a practical case study focused on the use of unmanned aerial systems for public safety and empirically study policy performance in myriad Erdös-Rényi settings.

Keywords:

Decision Analysis, Online Learning, Sequential Decision Theory, Stochastic Optimization, Longest Path Problem

1. Introduction

A traveler knows the adjacency matrix of a graph and the vertex at which he is located. Each time an edge is traversed, there is a cost. When a new node is reached, there is a reward. The costs and rewards are unknown, but the traveler is a Bayesian with a joint prior distribution over them. If the traveler backtracks over an edge, the previous cost is assessed, but node rewards are only received once. Adopting decision-analytic principles, the traveler stops when the future expected utility is negative or a fixed number of decisions has been made.

This class of problems is quite general and captures many situations in sequential decision making. One has prior beliefs, makes a choice, observes the results, updates the prior, and then makes another decision. Such a structure, as well as the network-traversal application, relates it to the Canadian Traveler Problem [27, 35] as well as the uncertain vehicle-routing work of Han et al. [15] and the research of Borrero et al. [5] on shortest-path interdiction with incomplete information, among others. However, the

generality of our problem links it to many settings beyond transportation, e.g., choosing a career path, portfolio management, and staged investments [22, 38]. This feature is due to the formulation embedding an information collection problem within a routing problem.

Ideally, the traveler's policy would map all locations and belief states to an optimal action. This ideal requires examination of all possible walks (i.e., a connected sequence of nodes) that start at his current location and determining their effects on his posterior beliefs given the observed costs and rewards. But, as we will see, such a solution is intractable. Even if edge costs and node rewards were known with certainty (i.e., perfect information is available), the problem is NP-hard. Therefore, we describe strategies that scale to larger networks and which approximate the optimal solution.

Related work in Ryzhov and Powell [31] solves a similar problem but assumes learning occurs before the traveler's route selection (i.e., offline). It distinguishes the information collection and decision phases with emphasis on the efficacy of the knowledge-gradient policy in the first phase. Ryzhov and Powell [32] expand this work to general linear programming problems. In contrast, this paper addresses online learning, in which the information collection and decision phases are intertwined; the traveler learns about the graph while interacting with it. This perspective aligns with that of Thul and Powell [40], which examines the routing of drones for forest-fire mitigation efforts.

Our work is also related to other stochastic network problems [e.g., see 8, 24]; a comprehensive review of such problems is provided by Powell et al. [30]. Particularly relevant is the body of research on the stochastic vehicle routing problems [e.g., see 33, 4, 36], as well as more recent work on the online shortest path [e.g., see 21] and the information-collection vehicle routing problems [e.g., see 2]. Although related, our underlying modeling framework is derived from the partially observed Markov decision processes of Aksakalli et al. [1] as well as the belief state representation of Powell [29]. Moreover, we note that our work is adjacent to typical Bayesian optimization approaches in its use of Gaussian process priors [34, 12]; however, it diverges since information collection is constrained by the graph's structure, thereby paralleling, to a degree, exotic Bayesian optimization problems [e.g., see 13].

In Section 2, we define the problem using the universal framework of Powell [28]; we also discuss assumptions on the traveler's prior. In Section 3, we set aside the information collection stage to derive the computational difficulties a clairvoyant traveler faces even with perfect information. This analysis gives insight into the structure of the traveler's optimal walk. Using this analysis, Section 4 provides a collection of policies the traveler may use to solve the problem. These policies are tested empirically in Section 5. Section 6 summarizes our findings.

2. The Traveler's Problem

The traveler's known, undirected graph is $\mathcal{G} = (\mathcal{N}, \mathcal{E})$, with \mathcal{N} the node set and \mathcal{E} the edge set. Edge-traversal costs are incurred every time an edge is crossed in either direction; node rewards accrue only on the first visit. Both are unknown, but we assume that they are functions of known covariates, $\mathbf{x}_e \in \mathbb{R}^M$, $e \in \mathcal{E}$ and $\mathbf{y}_i \in \mathbb{R}^N$, $i \in \mathcal{N}$, where

M indicates the number of edge features and N indicates the number of node features. The edge-traversal costs are an unknown function $c(\mathbf{x}_e)$, and the node rewards are an unknown function $r(\mathbf{y}_i)$. We assume that each node has a self-edge with zero cost traversal; this allows travel to stop under a fixed time horizon. Also, we alias (i, j) and (j, i), using both terms to refer to the same edge. Utility is assumed to accumulate additively based upon the difference between reward and cost; therefore, to maintain focus on the underlying dynamics, we often refer to utility as net qain.

Under these conditions, the traveler wants to identify an expected-utility-maximizing walk through the graph from some $i_0 \in \mathcal{N}$. However, due to the unknown functions $c(\mathbf{x}_e)$ and $r(\mathbf{y}_i)$, the traveler's decisions are coupled with his subjective beliefs. Since the traveler learns about these functions while traversing the network, his decisions depend on both his location and belief state, implying that the traveler's behavior is best determined by a policy. Assuming independent Gaussian process priors over c and r, we present a tractable formulation of the traveler's problem using the framework in Powell [28]. Policies for this problem are given in Section 4.

2.1. The Traveler's Prior Beliefs

We assume independent $c \sim \mathcal{GP}(\mu_c, \Sigma_c)$ and $r \sim \mathcal{GP}(\mu_r, \Sigma_r)$ where μ_c and μ_r are mean functions from $\mathbb{R}^M \to \mathbb{R}$ and $\mathbb{R}^N \to \mathbb{R}$, respectively, and Σ_c and Σ_r are their corresponding covariance functions. For a Gaussian process, any finite collection of its unknown realizations has a multivariate normal distribution. Also, the posterior of a Gaussian process given an observation is also a Gaussian process. These properties enable computation of the traveler's posterior beliefs given observed costs and rewards.

Consider the prior distribution over k unobserved edge-traversal costs; denote the sequences of edges as $e_{1:k} = (e_1, \dots, e_k)$. Then the prior over $c(\mathbf{x}_{e_{1:k}}) = [c(\mathbf{x}_{e_1}), \dots, c(\mathbf{x}_{e_k})]$ is

$$c\left(\mathbf{x}_{e_{1:k}}\right) \sim \text{Normal}\left(\mu_{c}\left(\mathbf{x}_{e_{1:k}}\right), \Sigma_{c}\left(\mathbf{x}_{e_{1:k}}, \mathbf{x}_{e_{1:k}}\right)\right).$$

We mirror the notation used by Frazier [11] for a function applied to a collection of points. That is, $\mathbf{x}_{e_{1:k}}$ indicates a sequence of feature vectors $\mathbf{x}_{e_1}, \dots, \mathbf{x}_{e_k}$; $\mu_c(\mathbf{x}_{e_{1:k}}) = [\mu_c(\mathbf{x}_{e_1}), \dots, \mu_c(\mathbf{x}_{e_k})]^{\top}$ is a mean vector, and $\Sigma_c(\mathbf{x}_{e_{1:k}}, \mathbf{x}_{e_{1:k}}) = [\Sigma_c(\mathbf{x}_{e_1}, \mathbf{x}_{e_1}), \dots, \Sigma_c(\mathbf{x}_{e_1}, \mathbf{x}_{e_k}); \dots; \Sigma_c(\mathbf{x}_{e_k}, \mathbf{x}_{e_1}), \dots, \Sigma_c(\mathbf{x}_{e_k}, \mathbf{x}_{e_k})]$ is a covariance matrix. Since $c(\mathbf{x}_{e_{1:k}})$ is multivariate normal, the posterior on $c(\mathbf{x}_{e_k})$ given the data $\mathbf{x}_{e_{1:k-1}}$ is univariate normal with

$$c(\mathbf{x}_{e_k}) \sim \text{Normal}\left(\mu_c(\mathbf{x}_{e_k}), \sigma_c^2(\mathbf{x}_{e_k})\right)$$
 (1)

where

$$\begin{split} &\mu_{c}\left(\mathbf{x}_{e_{k}}\right) = \Sigma_{c}\left(\mathbf{x}_{e_{k}}, \mathbf{x}_{e_{1:k-1}}\right) \Sigma_{c}\left(\mathbf{x}_{e_{1:k-1}}, \mathbf{x}_{e_{1:k-1}}\right)^{-1} \left(c(\mathbf{x}_{e_{1:k-1}}) - \mu_{c}(\mathbf{x}_{e_{1:k-1}})\right) + \mu_{c}\left(\mathbf{x}_{e_{k}}\right), \\ &\sigma_{c}^{2}\left(\mathbf{x}_{e_{k}}\right) = \Sigma_{c}(\mathbf{x}_{e_{k}}, \mathbf{x}_{e_{k}}) - \Sigma_{c}\left(\mathbf{x}_{e_{k}}, \mathbf{x}_{e_{1:k-1}}\right) \Sigma_{c}\left(\mathbf{x}_{e_{1:k-1}}, \mathbf{x}_{e_{1:k-1}}\right)^{-1} \Sigma_{c}\left(\mathbf{x}_{e_{1:k-1}}, \mathbf{x}_{e_{k}}\right). \end{split}$$

The posterior for multiple unobserved edges, $e_{k:K}$, is

$$c\left(\mathbf{x}_{e_{k:K}}\right) \sim \text{Normal}\left(\mu_c\left(\mathbf{x}_{e_{k:K}}\right), \text{cov}_c\left(\mathbf{x}_{e_{k:K}}\right)\right)$$
 (2)

where

$$\mu_c\left(\mathbf{x}_{e_{k:K}}\right) = \Sigma_c\left(\mathbf{x}_{e_{k:K}}, \mathbf{x}_{e_{1:k-1}}\right) \Sigma_c\left(\mathbf{x}_{e_{1:k-1}}, \mathbf{x}_{e_{1:k-1}}\right)^{-1} \left(c\left(\mathbf{x}_{e_{1:k-1}}\right) - \mu_c\left(\mathbf{x}_{e_{1:k-1}}\right)\right) + \mu_c\left(\mathbf{x}_{e_{k:K}}\right),$$

$$\operatorname{cov}_c\left(\mathbf{x}_{e_{k:K}}\right) = \Sigma_c\left(\mathbf{x}_{e_{k:K}}, \mathbf{x}_{e_{k:K}}\right) - \Sigma_c\left(\mathbf{x}_{e_{k:K}}, \mathbf{x}_{e_{1:k-1}}\right) \Sigma_c\left(\mathbf{x}_{e_{1:k-1}}, \mathbf{x}_{e_{1:k-1}}\right)^{-1} \Sigma_c\left(\mathbf{x}_{e_{1:k-1}}, \mathbf{x}_{e_{k:K}}\right).$$

Similarly, conditional on the payoffs from the observed nodes, the posterior on the unobserved nodes is

$$r(\mathbf{y}_{j_{l:L}}) \sim \text{Normal}(\mu_r(\mathbf{y}_{j_{l:L}}), \text{cov}_r(\mathbf{y}_{j_{l:L}}))$$
 (3)

where $j_{1:l}$ is a sequence of l nodes, $\mathbf{y}_{j_{1:l-1}}$ and $r(\mathbf{y}_{j_{1:l-1}})$ are observed, and μ_r and cov_r are analogously defined. We shall use these posterior distributions to solve the traveler's problem in Section 4.

Unlike other applications of Gaussian processes (e.g., Bayesian optimization), c and r cannot be queried at an arbitrary feature vector. The traveler can only observe the functions at a new feature vector if it corresponds to a node/edge adjacent to his current position. This fact, coupled with the traveler's objective to maximize his net gain, complicates the problem and distinguishes it from other knowledge acquisition settings.

2.2. Problem Formulation under a Gaussian Process Prior

We present a formulation for the traveler's problem that simultaneously characterizes the knowledge acquisition and reward-accrual dynamics. It uses the universal framework of Powell [28] for sequential decision making, which includes explicitly defined state variables, decision variables, exogenous information, a state-transition model, and an objective function. There is a slight deviation from the standard notation in order to accommodate conventions in graph theory and statistics.

Let $\mathcal{T} = \{0, 1, ..., T\}$ denote the set of decision epochs. Each decision epoch $t \in \mathcal{T}$ represents a particular point in time at which the traveler makes a decision.

2.2.1. State Variables

State variables describe the traveler's location and beliefs at a given time. This information is necessary and sufficient to compute the traveler's net gain at time t and to derive the transition model that updates the information needed for decisions at time t+1.

At some time t, the traveler must decide which edge to traverse to reach the next node, or whether to terminate the exploration. By equations (1)–(3), his beliefs at time t are determined from all previously observed data, as well as his prior mean and covariance functions. Because the latter two functions characterize the traveler's prior beliefs, this implies that the state variables can be defined as the tuple

$$S_t = \langle i_t, \mathcal{I}_t, \mathcal{C}_t, \mathcal{R}_t \rangle$$

where i_t is the traveler's current location, \mathcal{I}_t lists the visited nodes, \mathcal{C}_t contains all observed \mathbf{x}_{e_k} and $c(\mathbf{x}_{e_k})$ pairs, and \mathcal{R}_t contains all observed \mathbf{y}_{j_l} and $r(\mathbf{y}_{j_l})$ pairs.

Different indices are used for \mathbf{x}_{e_k} and \mathbf{y}_{j_l} because, depending upon \mathcal{I}_t , not all sampled \mathbf{x} - or \mathbf{y} -values will yield a new observation. If node j_t has already been visited then its $r(\mathbf{y}_{j_t})$ is already known. But if (i_t, j_t) has not yet been traversed, observing it provides new information on c.

2.2.2. Decision Variables

At time t, the traveler must choose which node j_t to visit from his current position i_t . The traveler's choice j_t must be in $\mathcal{N}(i_t) \cup \{i_t\}$ such that $\mathcal{N}(i_t)$ is the set of all nodes adjacent to i_t . If $j_t = i_t$, the traveler stays in place.

2.2.3. Exogenous Information

Given the decision j_t , the exogenous information is determined by the covariates associated with both j_t and $e_t = (i_t, j_t)$. Namely, if j_t has not yet been visited, the traveler observes the values of the unknown functions at this input, i.e., $c(\mathbf{x}_{e_t})$ and $r(\mathbf{y}_{i_t})$. Alternatively, if j_t has been visited but e_t has not been traversed, the traveler only sees $c(\mathbf{x}_{e_t})$ because no reward is received. If the traveler crosses a previously traversed edge, no new information is observed; the known travel cost for $c(\mathbf{x}_{e_t})$ accrues and no node reward is received.

2.2.4. Transition Model

After having made decision j_t and observing $c(\mathbf{x}_{e_t})$ and $r(\mathbf{y}_{j_t})$, the state variables update to enable the tractable modeling of the traveler's next decision. In this setting, the transition model simply involves moving the traveler to his new location and appending information to the relevant sets. Therefore, after making a decision j_t and observing the exogenous information, the new state becomes

$$S_{t+1} = \langle j_t, \mathcal{I}_{t+1}, \mathcal{C}_{t+1}, \mathcal{R}_{t+1} \rangle.$$

where

$$\mathcal{I}_{t+1} = \begin{cases}
\mathcal{I}_t \cup \{j_t\}, & j_t \notin \mathcal{I}_t, \\
\mathcal{I}_t, & j_t \in \mathcal{I}_t,
\end{cases}$$

$$\mathcal{C}_{t+1} = \begin{cases}
\mathcal{C}_t \cup \{(\mathbf{x}_{e_t}, c(\mathbf{x}_{e_t}))\}, & (\mathbf{x}_{e_t}, c(\mathbf{x}_{e_t})) \notin \mathcal{C}_t, \\
\mathcal{C}_t, & (\mathbf{x}_{e_t}, c(\mathbf{x}_{e_t})) \in \mathcal{C}_t,
\end{cases}$$
(5)

$$C_{t+1} = \begin{cases} C_t \cup \{(\mathbf{x}_{e_t}, c(\mathbf{x}_{e_t}))\}, & (\mathbf{x}_{e_t}, c(\mathbf{x}_{e_t})) \notin C_t, \\ C_t, & (\mathbf{x}_{e_t}, c(\mathbf{x}_{e_t})) \in C_t, \end{cases}$$
(5)

$$\mathcal{R}_{t+1} = \begin{cases}
\mathcal{R}_t \cup \{(\mathbf{y}_{j_t}, r(\mathbf{y}_{j_t}))\}, & (\mathbf{y}_{j_t}, r(\mathbf{y}_{j_t})) \notin \mathcal{R}_t, \\
\mathcal{R}_t, & (\mathbf{y}_{j_t}, r(\mathbf{y}_{j_t})) \in \mathcal{R}_t.
\end{cases}$$
(6)

2.2.5. Objective Function

Ideally, the traveler would design a policy that maximizes his total net gain based on the fact that any given decision j_t is associated with a net gain determined by its underlying features, i.e.,

$$g(S_t, j_t) = \begin{cases} r(\mathbf{y}_{j_t}) - c(\mathbf{x}_{e_t}), & j_t \notin \mathcal{I}_t, \\ -c(\mathbf{x}_{e_t}), & j_t \in \mathcal{I}_t \setminus \{i_t\}, \\ 0, & j_t = i_t. \end{cases}$$
(7)

However, since no $c(\mathbf{x}_{et})$ and $r(\mathbf{y}_{jt})$ are observed at the start of travel (i.e., t = 0), the traveler's objective is to maximize his expected total net gain. His optimization problem is therefore to identify a policy that solves

$$\max_{\pi \in \Pi} \mathbb{E} \left[\sum_{t \in \mathcal{T}} g\left(S_t, J^{\pi}(S_t)\right) \right],$$

where $J^{\pi}(S_t)$ is a decision function that returns j_t based on the policy π , and Π is the family of feasible policies under consideration. The expectation is calculated using the traveler's subjective beliefs as described in Section 2.1.

3. Problem Insights from a Clairvoyant Traveler

The traveler's problem is complicated by the uncertainty about the node rewards and edge costs and by the combinatorial nature of the action space. Therefore, to inform policy design, we isolate the combinatorial challenge by considering a clairvoyant traveler who has perfect knowledge about the graph, costs, and rewards. This clairvoyant seeks to plan a walk that maximizes his net gain.

The clairvoyant's problem is related to the longest-path problem [20]. This relationship can be seen by transforming \mathcal{G} into a directed graph and adding the node reward to each of its edges. Directed edges are necessary because, depending upon the direction in which an edge is traversed, the net gain may be distinct based on the different destination node rewards. The clairvoyant need not consider the features \mathbf{x}_e and \mathbf{y}_j since the rewards and costs are known. Therefore, by setting all node rewards to zero and the edge weights to $r_j - c_{(i,j)}$ where $r_j \geq 0$ is the known reward for node j and $c_{(i,j)} \geq 0$ is the known traversal cost for directed edge (i,j), the structural similarity of the clairvoyant's problem to the longest-path problem is clear.

However, unlike the longest-path problem, the clairvoyant's edge weights are not static. After node j has been visited, the weights update to $-c_{(i,j)}$. Unfortunately, this additional structure does not reduce the computational complexity.

The decision variant of the clairvoyant's problem asks whether there exists a walk yielding some pre-specified reward. Allowing this reward to equal $|\mathcal{N}|$, Property 1 shows that, like the longest-path problem, finding the Hamiltonian path reduces to the clairvoyant's problem [20]. The existence of such a Karp reduction [e.g., see 41] implies the clairvoyant's problem is intractable.

Property 1. The clairvoyant's decision problem is NP-hard.

Proof: Take a Hamiltonian path problem on an undirected graph $\mathcal{H} = (\mathcal{N}_{\mathcal{H}}, \mathcal{E}_{\mathcal{H}})$. Build a polynomial time reduction to the clairvoyant's problem as follows: add a fully connected node i_0 with $c_{(i_0,j)} = 0$, $\forall j \in \mathcal{N}_{\mathcal{H}}$ and $r_{i_0} = 0$. Let i_0 be the clairvoyant's starting point, and set $c_{(i,j)} = 1$, $\forall (i,j) \in \mathcal{E}_{\mathcal{H}}$ and $r_i = 2$, $\forall i \in \mathcal{N}_{\mathcal{H}}$. Call the new graph $\mathcal{G} = (\mathcal{N}, \mathcal{E})$.

A Hamiltonian path solves the clairvoyant's problem: Given a valid Hamiltonian path ρ on \mathcal{H} , let him walk through \mathcal{G} , moving from i_0 to the endpoint of ρ . Since $|\mathcal{N}_H| = |\mathcal{N}| - 1$, this walk earns a reward of $2(|\mathcal{N}| - 1) - (|\mathcal{N}| - 2) = |\mathcal{N}|$, indicating a solution to the clairvoyant's decision problem.

The solution to the clairvoyant's problem is a Hamiltonian path: Assume his walk on \mathcal{G} has reward $|\mathcal{N}|$. Such a walk cannot revisit a node, else its payoff is less than $|\mathcal{N}|$. Therefore, since traveling from i_0 to an unvisited node along ρ yields a net gain of 2, and traveling to a unvisited node in ρ from another along ρ yields a net gain of 1, the clairvoyant's walk, excluding i_0 , is a Hamiltonian path on \mathcal{H} .

Property 1's computational challenge for the clairvoyant applies to the traveler's problem in Section 2. If the traveler is at i_t , he will seek an expected-utility-maximizing walk in the same manner as the clairvoyant. This strategy is common in sequential decision problems but it is NP-hard in the traveler's setting.

Additional analysis of the clairvoyant's problem reveals that the network's payment structure ensures some walks are never optimal. Properties 2 and 3 provide simple but useful results that reduce the clairvoyant's decision space. Moreover, these results also ensure that an optimal walk of finite length always exists. Properties 2 and 3 directly extend to the traveler's problem by replacing random edge costs and node rewards with their expectations.

Let a circuit ξ on \mathcal{G} be a sequence of edges in which the first and last nodes are identical. Nodes in a circuit may be repeated but edges may not. Let \mathcal{N}_{ξ} be the set containing distinct nodes visited in ξ . The following properties can be derived.

Property 2. The clairvoyant's optimal walk does not repeat the same circuit.

Proof: Once a circuit is traversed, all its node rewards are collected. Repeating the circuit yields a negative net gain and returns the traveler to the same location.

Property 3. If there exists distinct circuits ξ_1 and ξ_2 , with the same end point and $\mathcal{N}_{\xi_1} \subset \mathcal{N}_{\xi_2}$, ξ_1 and ξ_2 cannot both be traversed on the clairvoyant's optimal walk.

Proof: Since

$$\begin{split} \sum_{i \in \mathcal{N}_{\xi_2}} r_i - \sum_{(i,j) \in \xi_1 \cap \xi_2} c_{(i,j)} - \sum_{(i,j) \in \xi_2 \setminus \xi_1} c_{(i,j)} > \sum_{i \in \mathcal{N}_{\xi_2}} r_i - 2 \sum_{(i,j) \in \xi_1 \cap \xi_2} c_{(i,j)} \\ - \sum_{(i,j) \in \xi_1 \setminus \xi_2} c_{(i,j)} - \sum_{(i,j) \in \xi_2 \setminus \xi_1} c_{(i,j)}, \end{split}$$

it is more profitable to take only ξ_2 than both ξ_1 and ξ_2 . And if

$$\sum_{i \in \mathcal{N}_{\xi_2} \backslash \mathcal{N}_{\xi_1}} r_i - \sum_{(i,j) \in \xi_2 \ \backslash \xi_1} c_{(i,j)} < - \sum_{(i,j) \in \xi_1 \backslash \xi_2} c_{(i,j)}$$

then it is more profitable to traverse ξ_1 than ξ_2 .

Properties 2 and 3 apply to any circuit, whether or not interior nodes are visited more than once. However, for circuits without repeated interior nodes, i.e., cycles, stronger results about the clairvoyant's optimal path can be derived. For large graphs, it is computationally burdensome to enumerate all cycles; however, they are characterized by a cycle basis. All cycles in \mathcal{G} can be formed by symmetric differences of its basis cycles. Polynomial time algorithms exist to find such cycle bases under relatively mild assumptions [i.e., see 16]. But regardless of how it is computed, once a cycle basis is provided, the following results apply to the clairvoyant's optimal path.

Property 4. Any edge (i, j) not present in a basis cycle of \mathcal{G} is traversed at most twice in the clairvoyant's optimal walk.

Proof: If (i, j) is not present in the cycle basis, it is not part of any cycle in \mathcal{G} . This implies (i, j) is a bridge connecting two node sets that become disjoint if the edge were deleted. Call these node subsets \mathcal{N}_1 and \mathcal{N}_2 such that $\mathcal{N} = \mathcal{N}_1 \cup \mathcal{N}_2$.

Without loss of generality, consider a finite walk w_1 with edge (i, j) repeated K times such that $i_0 \in \mathcal{N}_1$. Since (i, j) is a bridge, we can write $w_1 = (w_{1,1}, (i, j), w_{1,2}, (i, j), ..., (i, j), w_{1,K+1})$ where $w_{1,k}$ are walks contained within w_1 . Note that $w_{1,k}$ only includes nodes in \mathcal{N}_1 when k is odd, and \mathcal{N}_2 otherwise. Likewise, for odd k > 1, the end points of $w_{1,k}$ are i, and for even k < K + 1, the end points of $w_{1,k}$ are j.

If K > 2 is odd then K + 1 is even, the walk w_1 terminates in \mathcal{N}_2 , and we can construct a new walk $w_2 = \{w_{1,1}, w_{1,3}, ..., w_{1,K}, (i,j), w_{1,2}, w_{1,4}, ..., w_{1,K+1}\}$. This new walk visits the same nodes as w_1 , but crosses (i,j) only once, implying the total edge cost of w_2 is less than w_1 . If K > 2 is even, we can similarly construct $w_2 = \{w_{1,1}, w_{1,3}, ..., w_{1,K-1}, (i,j), \rho_{1,2}, \rho_{1,4}, ..., \rho_{1,K}, (i,j), \rho_{1,K+1}\}$ such that the cost of w_2 is less than that of w_1 . Therefore, if K > 2, another walk of lesser cost can always be constructed.

Property 4 implies that, if \mathcal{G} contains a bridge, the clairvoyant can identify a large number of solutions that are dominated by the walk's structure alone. As the number of bridges in \mathcal{G} increases, so too does the number of walks that can be discarded. A graph that maximally exhibits this property only includes edges that are bridges and, by definition, is acyclic. Property 4 can be extended in such situations to generate further conditions on the clairvoyant's optimal walk.

Property 5. If G is acyclic, the number of times the clarivoyant visits a node on his optimal walk is bounded above by two times the node's degree.

Proof: If \mathcal{G} is acyclic, its cycle basis is empty and contains no edges. By Property 4, this implies every edge $(i,j) \in \mathcal{E}$ is traversed no more than twice. Therefore, any node $i \in N$ can be visited no more than two times its degree.

Property 6. If \mathcal{G} is acyclic, the clarivoyant's optimal walk does not exceed length $2|\mathcal{E}|$.

Proof: A walk of greater length implies some $i \in N$ was visited more than two times its degree, thereby violating Property 5.

Property 6 provides an upper-bound on how many steps into the future the clairvoyant must plan in order to identify an optimal solution. But the results rely upon an acylic \mathcal{G} . Other properties enable upper bounds for general graphs, but with substantially more effort. The clairvoyant would need to account for all circuits associated with each node and determine which are dominated, and the effort to identify such bounds may exceed their utility.

Properties 5 and 6 imply that efficient algorithms may exist for the clairvoyant's problem when \mathcal{G} is acyclic. Property 1 ensures that, for general graphs, the problem is difficult to solve. These results directly apply to the traveler's problem and to his corresponding policy design. On a general graph, optimal decisions are too computationally difficult to identify.

4. Solving the Traveler's Problem

Using the results from Section 3, we examine four heuristic policies to solve the traveler's problem. These policies rely upon the traveler's belief at time t, which is calculated using Equations (1) through (3). At each new state S_t , the policy's associated decision function is used to determine the traveler's action based on his updated beliefs. Each policy is based on the similarity of the traveler's problem to the longest-path problem; however, they differ in how they compute forecasts of a decision's expected future returns.

4.1. Myopic Baseline Policy

The myopic policy (i.e., policy M) is the baseline used for comparative analysis. This policy centers on the immediate outcomes of a given decision j_t , disregarding the potential long-term effects. Policy M transitions from node i_t to j_t via the following decision function:

$$J^{M}(S_{t}) = \underset{j_{t} \in \mathcal{N}(i_{t})}{\operatorname{arg max}} \mathbb{E}\left[g\left(S_{t}, j_{t}\right)\right], \tag{8}$$

where $\mathcal{N}(i_t)$ is the set of nodes adjacent to i_t . The expectation is taken using the posterior distributions over $c(\mathbf{x}_{e_t})|\mathcal{C}_t$ and $r(\mathbf{y}_{j_t})|\mathcal{R}_t$. Since both $r(\mathbf{y}_{j_t})|\mathcal{R}_t$ and $c(\mathbf{x}_{e_t})|\mathcal{C}_t$ are independent and normally distributed, it immediately follows that

$$\mathbb{E}\left[g\left(S_{t}, j_{t}\right)\right] = \begin{cases} \mu_{r|\mathcal{R}_{t}}(\mathbf{y}_{j_{t}}) - \mu_{c|\mathcal{C}_{t}}(\mathbf{x}_{e_{t}}), & j_{t} \notin \mathcal{I}_{t}, \\ -\mu_{c|\mathcal{C}_{t}}(\mathbf{x}_{e_{t}}), & j_{t} \in \mathcal{I}_{t} \setminus \{i_{t}\}, \\ 0, & j_{t} = i_{t}. \end{cases}$$
(9)

The myopic policy is exploitative, focusing only on immediate expected rewards without considering variability. In the context of this research, the myopic policy may be suitable when dense network connections make long-term computations expensive, or when node

rewards substantially exceed edge-traversal cost, thereby reducing the need for exploring future states and alternative actions.

4.2. Upper Confidence Bound Policy

The upper confidence bound (UCB) policy (i.e., policy UCB) is based on an exploration-exploitation trade-off. It modifies the traditional multi-arm bandit problem to suit our setting. The idea is to balance the trade-off between choosing actions that the agent knows yield good rewards (exploitation) and taking a risk by trying actions that the traveler has not explored much (exploration) to possibly find better solutions. The UCB algorithm deals with this trade-off by favoring actions that are both rewarding and less explored. Specifically, the UCB policy transitions from node i_t to j_t via the following decision function:

$$J^{UCB}(S_t|\lambda) = \underset{j_t \in \mathcal{N}(i_t)}{\operatorname{arg max}} \mathbb{E}\left[g\left(S_t, j_t\right)\right] + \lambda \mathbb{V}\left[g\left(S_t, j_t\right)\right], \tag{10}$$

where $\lambda \geq 0$ is a tunable exploration parameter. As indicated in the previous section, $r(\mathbf{y}_{j_t})|\mathcal{R}_t$ and $c(\mathbf{x}_{e_t})|\mathcal{C}_t$ are independent and normally distributed. This allows us to generate the cases provided in Equation (9) as well as the following:

$$\mathbb{V}\left[g\left(S_{t},j_{t}\right)\right] = \begin{cases} \sigma_{r|\mathcal{R}_{t}}^{2}(\mathbf{y}_{j_{t}}) + \sigma_{c|\mathcal{C}_{t}}^{2}(\mathbf{x}_{e_{t}}), & (\mathbf{x}_{e_{t}},r(\mathbf{y}_{j_{t}})) \notin \mathcal{R}_{t}, (\mathbf{x}_{e_{t}},c(\mathbf{x}_{e_{t}})) \notin \mathcal{C}_{t}, \\ \sigma_{c|\mathcal{C}_{t}}^{2}(\mathbf{x}_{e_{t}}), & (\mathbf{x}_{e_{t}},r(\mathbf{y}_{j_{t}})) \in \mathcal{R}_{t}, (\mathbf{x}_{e_{t}},c(\mathbf{x}_{e_{t}})) \notin \mathcal{C}_{t}, \\ \sigma_{r|\mathcal{R}_{t}}^{2}(\mathbf{y}_{j_{t}}), & (\mathbf{x}_{e_{t}},r(\mathbf{y}_{j_{t}})) \notin \mathcal{R}_{t}, (\mathbf{x}_{e_{t}},c(\mathbf{x}_{e_{t}})) \in \mathcal{C}_{t}, \\ 0, & (\mathbf{x}_{e_{t}},r(\mathbf{y}_{j_{t}})) \in \mathcal{R}_{t}, (\mathbf{x}_{e_{t}},c(\mathbf{x}_{e_{t}})) \in \mathcal{C}_{t}. \end{cases}$$

$$(11)$$

Different values of λ cause different traveler choices. If $\lambda=0$, the traveler ignores the uncertainty in his estimate and moves to the node with the largest, immediate, expected net gain. It is equivalent to using the myopic policy. But if λ is relatively large, it strongly encourages exploration, potentially forgoing immediate rewards but possibly leading to better long-term outcomes as it discovers higher-reward actions. The ideal λ value depends on the specific environment and the problem at hand, balancing between immediate and future rewards.

4.3. H-Path Policy

The H-path policy (i.e., policy HP) is a rolling horizon policy, choosing an action based on a preferred path of length H from i_t . Using the information at S_t , policy HP picks a preferred path and the traveler moves to the first node on that path. Upon reaching the new node, the traveler updates his priors and identifies a new preferred path of length H and repeats the selection process.

Similar to policy UCB, the H-path policy chooses actions by balancing the expected

net gain against the reduction in uncertainty. It finds path $e_{1:H}^*$ from i_t by solving

$$\mathbf{P1}: \max_{\substack{e'_{1:H} \in \mathcal{P}_{H}(i_{t}) \\ j'_{k} = d(e'_{k}), \ \forall k}} \mathbb{E}\left[\sum_{k=1}^{H} g\left(S'_{k}, j'_{k}\right)\right] + \alpha\left(\mathbb{V}_{G}\left[c\left(\mathbf{x}_{e'_{1:H}}\right) \middle| \mathcal{C}_{t}\right] + \mathbb{V}_{\mathbb{G}}\left[r\left(\mathbf{y}_{j'_{1:H}}\right) \middle| \mathcal{R}_{t}\right]\right),$$

where $S'_{1:H}$ is a sequence of synthetic states, $e'_{1:H}$ is a candidate path of length H from i_t , $\mathcal{P}_H(i_t)$ is the set of all H-length paths from i_t , $j'_k = d(e'_k)$ such that $d(\cdot)$ provides the destination (tail) of an edge, α is a tunable exploration parameter, and \mathbb{V}_G is the generalized variance (a scalar measure of multidimensional scatter). The smaller the value of \mathbb{V}_G , the more association exists between the variables, so observed variables lead to greater reduction in uncertainty for the unobserved. For large H, the feasible region of Problem P1 will contain many paths; however, depending upon the structure of \mathcal{G} , Properties 2 – 6 help discard solutions based upon the already traversed walk.

Notably, the transition model for the synthetic future states differs slightly from that discussed in Section 2; i.e., $S'_1 = S_t$, $S'_{k+1} = \langle j'_k, \mathcal{I}'_k, \mathcal{C}_t, \mathcal{R}_t \rangle$ for k < H, and \mathcal{I}'_{k+1} is updated similarly to equation (4). Therefore, only the traveler's position and history of visited nodes are updated. However, since revisiting nodes is prohibited on paths, if the decision space is properly constrained, one may forgo updating \mathcal{I}_k as well.

By the linearity of expectation and the definition of generalized variance [3], the expectation in Problem P1 can be simplified using Equation (9)

$$\mathbb{V}_{G}\left[c\left(\mathbf{x}_{e_{1:H}^{\prime}}\right)|\mathcal{C}_{t}\right] = \det\left(\operatorname{cov}_{c|\mathcal{C}_{t}}\left(\mathbf{x}_{e_{1:H}^{\prime}}\right)\right),$$

$$\mathbb{V}_{G}\left[r\left(\mathbf{x}_{j_{1:H}^{\prime}}\right)|\mathcal{R}_{t}\right] = \det\left(\operatorname{cov}_{r|\mathcal{R}_{t}}\left(\mathbf{y}_{j_{1:H}^{\prime}}\right)\right),$$

where these covariance matrices are defined in Section 2.1. Once Problem P1 is solved and the preferred path $e_{1:H}^*$ is identified, the H-path policy's decision rule dictates the traveler move along e_1^* to $d(e_1^*)$. Specifically, policy HP transitions from node i_t to j_t via the following decision function:

$$J^{HP}(S_t|\alpha, H) = d(e_1^*). \tag{12}$$

Unfortunately, depending on the structure of \mathcal{G} and the size of H, solving Problem P1 can be computationally intractable. It is an NP-Hard problem. To identify $e_{1:H}^*$ at any state S_t , the traveler must address a regularized, single-source, longest-path problem. While feasible for acyclic \mathcal{G} or small H values, complex graphs or large H-values require alternative methods to approximate the optimal solution of Problem P1.

We use a neighborhood search heuristic to approximate a solution to Problem P1, thereby facilitating the application of the H-path policy for general problems. This heuristic employs a 2-Opt-like technique, adapting a method frequently used to solve traveling salesman problems [17] whereby two edges on an existing walk are removed and the walk is reconnected with two new edges and their possible reordering. The algorithm for identifying this approximate solution, $\hat{e}_{1:H}$, is detailed in Algorithm 1.

Beginning with a feasible path $e'_{1:H}$, Algorithm 1 sequentially alters the path's visited

Algorithm 1 *H*-Path Neighborhood Search

```
1: Input: \mathcal{G}, \mu_c, \Sigma_c, \mu_r, \Sigma_r
```

2: Generate initial feasible path $e'_{1:H}$

3: while improvements can be made do

4: **for** each pair of adjacent edges in $e'_{1:H}$ **do**

5: remove the pair from $e'_{1:H}$

6: identify the first substitution pair that improves objective function

7: replace the removed pair with the identified substitution

8: end for

9: update $e'_{1:H}$ with the modified path

10: end while

11: **Output**: $J^{HP}(S_t|\alpha, H) = d(e'_1)$

nodes. It navigates to neighboring solutions in $\mathcal{P}_H(i_t)$ by removing two adjacent edges from $e'_{1:H}$ and substituting them with the first identified pair that results in a new path with a superior objective function value. The process continues iteratively with this new path, modifying all adjacent edges along the path until no further improvements can be found. Upon conclusion, the algorithm chooses an action tied to the first node in the walk linked with the optimized path $e'_{1:H}$.

4.4. Speculating Clairvoyant Policy

The speculating clairvoyant policy (i.e., policy SC) assumes that point estimates represent true values and constructs a policy mimicking the foresight of a clairvoyant. In this framework, when the traveler is at state S_t , the traveler's policy is constructed by using point estimates of the unknown parameters, and then solving the subsequent problem in a manner similar to a clairvoyant. The mean function estimates replace the unknowns in the graph, and, once the optimal clairvoyant solution is identified, the traveler progresses to the first node along this walk.

The traveler attempts to solve the following optimization problem and, akin to the H-path policy, moves to the first node along the associated walk. The problem is

$$\mathbf{P2}: \max_{\substack{e_{1:V}' \in \mathcal{W}_{V}(i_{t}) \\ j_{k}' = d(e_{k}'), \ \forall k}} \mathbb{E}\left[\sum_{k=1}^{V} g\left(S_{k}', j_{k}'\right)\right]$$

where V is a sufficiently large number (i.e., akin to the big-M method in linear programming; cf. Taha [39]), $W_V(i_t)$ denotes the set of all V-length walks from i_t , and the possible state transitions are identical to the H-path policy. Note that, in general, $\|W_V(i_t)\|$ can be large, but Properties 2 – 6 may be used to reduce its cardinality by discarding walks, depending upon the structure of \mathcal{G} (e.g., those repeating the same circuit many times). Once Problem P2 is solved, the associated decision rule is

$$J^{SC}(S_t) = d(e_1^*), (13)$$

such that $e_{1:V}^*$ is the optimal walk. Unfortunately, Property 1 shows that solving Problem

P2 is NP-hard, except for well-behaved graphs. Drawing on the parallels between the clairvoyant's problem and the longest path problem, we set forth a label-setting heuristic, inspired by the Bellman-Ford algorithm for the single-source, shortest-path problem, given in Algorithm 2.

Algorithm 2 Label-Setting Heuristic

```
Input: \mathcal{G}, S_t, \mu_c, \mu_r
Set \mathcal{E}_D to the directed equivalent of \mathcal{E}
for k = 1, ..., \beta do
 \Omega_k(i) = \{\}, \ \forall i \in \mathcal{N}
                                                                                        ➤ No predecessors assigned
 z_k(i_t) = 0
  z_k(i) = -\infty, \ \forall i \in \mathcal{N} \setminus i_t
 Randomly order \mathcal{E}_D to create \mathcal{E}'_D
 for n=1,...,N do
   for each (i, j) \in \mathcal{E}'_D do
     if j \notin \mathcal{I}_t and j \notin \Omega(i) then \delta = \mu_{r|\mathcal{R}_t}(y_j) - \mu_{c|\mathcal{C}_t}(x_{(i,j)})
     else \delta = -\mu_{c|\mathcal{C}_t}(x_{(i,j)})
     end if
     if z_k(i) + \delta > z_k(j) then
                                                                 > Associated walk yields a greater reward
       z_k(j) = z_k(i) + \delta
       \Omega_k(i) = \Omega_k(i) \cup \{i\}
     end if
   end for
 end for
end for
\{k^*, i^*\} = \arg\max_{k,i} z_k(i)
Set e'_{1:V} according to node order of \Omega_{k*}(i^*) with V = |\Omega_{k*}(i^*)|
Output: J^{SC}(S_t) = d(e'_1)
```

Algorithm 2 uses a modified Bellman-Ford routine within an inner search loop that is repeated β times. This inner search routine contrasts with the traditional Bellman-Ford algorithm via its labeling system and the direction of its inequalities. Here, labels encompass the entire sequence of visited predecessors during the walk. Classic assumptions, such as the prohibition against cycle traversal, no longer apply. Furthermore, while Bellman-Ford exclusively considers paths, Algorithm 2 is able to handle more diverse walks. But, in so doing, the order in which edges are searched plays a more prominent role, potentially leading the algorithm to converge to a local optimum. Therefore, to manage these disparities, Algorithm 2 incorporates a tuning parameter β and edge order randomization. Namely, the algorithm uses a different random seed for every iteration k to shuffle the order in which the edges are searched over the β iterations. It induces stochasticity, facilitates exploration, and allows computational effort to be tuned. Upon concluding the β iterations, the algorithm chooses an action tied to the first node in the walk linked with the maximum z_k -value.

5. Computational Experimentation

This section empirically explores the Bayesian graph traversal problem and examines the performance of the four previous policies. Section 5.1 considers an example that shows the results of each policy and compares their performance to the optimal walk of a clairvoyant. Section 5.2 further examines policy performance on a more complicated instance based upon a public-safety case study to illustrate the practical implications of the Bayesian graph traversal problem. Thereafter, Section 5.3 compares the policies to the myopic baseline on larger-scaled instances that cannot readily be solved, even by a clairvoyant. Random networks are generated based on the Erdös-Rényi model, and a full-factorial design over the parameters explores the effect of the network's structure on policy performance. All experiments and analyses are done on a dual Intel Xeon E5-2650v2 workstation with 128 GB of RAM using MATLAB. In all experiments, T=500 so that the time horizon is not a limiting factor.

5.1. Illustrative Example

We begin by comparing the myopic policy to the optimal clairvoyant solution. The problem involves a densely connected network of five nodes. Each node i is randomly situated within a two-dimensional Cartesian coordinate space of $(x_i, y_i) \in P$, where $P = \{(x, y) : 0 \le x, y \le 10\}$. The network structure is shown in Figure 1. For legibility, a node's self-edges are not depicted, but their use is implied when the traveler ceases to move.

Here, the node characteristics (features) are the node's degree and the average degree of its neighbors. A node's degree is its number of edges. The average neighbor degree, a metric employed in network structure analysis, reflects the connectivity of nodes linked to the given node. Edge features are the Cartesian coordinates of the nodes the edge connects. The node reward is derived from a second-order interaction model, with the first term as node degree, and the second as the average neighbor degree. The edge costs are a function of the Euclidean distance between linked nodes. Tables 1 and 2 show the features and rewards/costs for the nodes and edges, respectively.

| Label | Coordinates | Degree | Avg. Neighbor Degree | True Reward |
|-------|-------------|--------|----------------------|-------------|
| 1 | (3,3) | 5 | 4.33 | 0* |
| 2 | (2,0) | 4 | 4.40 | 61.36 |
| 3 | (10,7) | 5 | 4.33 | 74.78 |
| 4 | (0,2) | 3 | 4.00 | 44.00 |
| 5 | (8,1) | 4 | 4.40 | 61.36 |

Table 1: Node Details

The traveler's beliefs about these unknown functions are defined in Section 2.1. Drawing from the Bayesian optimization literature [12, 14], the prior mean functions are

^{*}Without loss of generality, the reward associated with the starting node is zeroed out

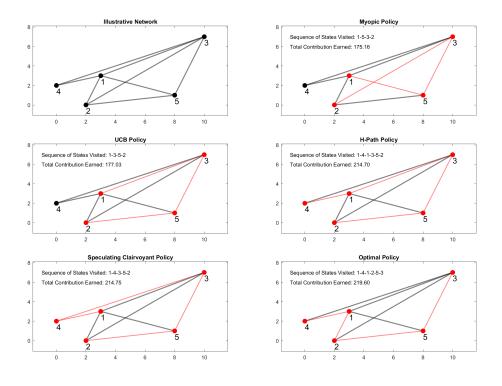


Figure 1: Illustrative Example - Policy Performance Comparison

Table 2: Edge Details

| Edges | True Cost |
|----------------------|-----------|
| $(1,2) \wedge (2,1)$ | 3.16 |
| $(1,3) \wedge (3,1)$ | 8.06 |
| $(1,4) \wedge (4,1)$ | 3.16 |
| $(1,5) \wedge (5,1)$ | 5.38 |
| $(2,3) \wedge (3,2)$ | 10.63 |
| $(2,5) \wedge (5,2)$ | 6.08 |
| $(3,4) \wedge (4,3)$ | 11.18 |
| $(3,5) \wedge (5,3)$ | 6.32 |

assumed to be constant. The mean functions for rewards and costs are the mean of all node rewards and edge-traversal costs. From Tables 1 and 2, the prior mean on the node rewards is 63.26, including the already-received reward from node one, and the prior mean on the edge costs is 6.75. So movement along the graph is generally profitable, and the myopic policy may perform relatively well.

For the covariance functions for rewards and costs, we use a Radial Basis Function (RBF) kernel with the bandwidth parameter set to one [i.e., see 7, 10, for more details]. This kernel implies that points near each other in the input space are highly correlated, capturing smooth transitions in our reward and cost structures across the network. Different mean and covariance functions can be explored, but the goal of this study is an initial analysis of the proposed policies under various algorithmic settings and problem characteristics. Parameter settings under consideration for policies UCB, HP, and SC are shown in Table 3. Algorithm 1 is used as an optimization routine to solve the subproblems for policy HP.

Figure 1 and Table 3 display the results. Figure 1 shows the routes taken by each policy on the network as well as the amount earned along the route. The optimal policy (i.e., the clairvoyant's route) has value 219.60. This value is as an upper bound on the traveler's net gain and is the reference point in Table 3. Policies M and UCB are comparable, both selecting a route with reward about 80% of the optimum. Neither performed any back-tracking nor did they revisit a node; however, the tendency of policy UCB to explore led it to find a somewhat better solution than the myopic policy. Policies HP and SC found comparable routes that were substantially better than the myopic policy, improving by approximately 23%. Both routes are nearly optimal; their optimality gaps are each less than 3%.

Table 3: Policy Settings and Performance Results

| Policy (π) | Parameter Setting(s) | Sequence of States Visited | Total Contribution Earned | Improvement over Myopic Policy | Percent Optimal |
|-------------------|-------------------------|-------------------------------|------------------------------|-----------------------------------|--------------------|
| M | - | 1-5-3-2 | 175.16 | - | 79.76% |
| UCB | $\lambda = 1$ | 1-3-5-2 | 177.03 | 1.07% | 80.61% |
| HP | $\alpha = 1; H = 3$ | 1-4-1-3-5-2 | 214.70 | 22.58% | 97.77% |
| SC | $\beta = 1$ | 1-4-3-5-2 | 214.75 | 22.60% | 97.79% |
| Optimal (π^*) | - | 1-4-1-2-5-3 | 219.60 | 25.37% | - |

Note that, in order to maximize his value, the traveler must backtrack across edge (1,4). However, backtracking behavior will never result from policies M or UCB; no reward is given for revisiting a node and no knowledge is obtained by recrossing an edge. Furthermore, revisiting a node via an untraversed edge is impossible in policy M and generally discouraged in policy UCB. The former is true because no reward is gained by revisiting a node, and the latter holds so long as little information is gained from crossing the untraversed edge. No such restrictions are present in policies HP and SC.

5.2. Case Study: UAS Operations for Public Safety

The results from the previous section lead us to explore how our policies might perform in a more realistic setting. Therefore, we perform an additional empirical exploration in a public-safety context. Specifically, we show how Bayesian graph traversal relates to the use of unmanned aerial systems (UASs) for first responders and how the policies can be used for that application.

Small UASs are increasingly viewed as force multipliers in public-safety operations. Their use has been advocated for law enforcement by the International Association of Chiefs of Police [18] to enhance situational awareness, investigate crime scenes, and respond quickly to disturbances while police officers are en route (e.g., via equipped two-communication). Similar capabilities have been promoted by the International Association of Fire Chiefs [19] for structural and wildland firefighting, among other disaster response operations. This first-responder demand has grown to such a degree that numerous companies (e.g., Skydio, UVT, Brinc) have emerged to satisfy it, and the National Urban Security Technology Laboratory [25], a subordinate unit of the US Department of Homeland Security, has published implementation recommendations. Notably, in any public-safety application, UASs must orient and route themselves within an uncertain environment, implying a Bayesian graph traversal problem.

To illustrate this connection, consider a police department in a standoff against criminals holding hostages on a compound. The compound contains three buildings and, although the police are uncertain of the configurations of the rooms, they have the blueprints of the structures. Hostage negotiators have been unsuccessful, so a SWAT team kinetic rescue operation is needed. The police have access to a drone with an on-board glass breaker (e.g., akin to the Brinc LEMUR) that is also equipped with other sensors (e.g., visible-light and thermal cameras). The police will use the drone to obtain information about the compound and the locations of the criminals and hostages, while minimizing the risk of detection risk. The police want the element of surprise and, if the criminals notice the drone's presence, their behavior may become erratic, threatening the lives of the hostages and compromising the SWAT team's objectives.

Figure 2 shows the information from the compound's blueprints. Nodes represent locations of interest, and edges represent possible connections between them. There are multiple doors and windows into each building; however, the police have identified three windows that the UAS could break with minimal noise (i.e., Nodes 8, 11, and 22). Prior to breaching a window, the police will create an auditory distraction so that traversing window edges is no more risky than traversing any other.

As in Section 5.1, node features consist of the node degree and the average neighbor degree. Thus, the police assume that rooms with heavier traffic contain more information than those less visited, and that the criminals' staging locations are based upon the compound design. Edge features are related to the Euclidean distance between the edge's tail and head with the assumption that longer transit times incur increased detection risk. The utility for rewards and costs is again assumed to be additive, with values assigned using the formulas in Section 5. Node rewards are formed using a second-order interaction model of the node features, and edge costs are a function of the Euclidean

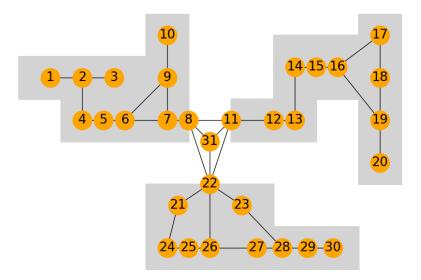


Figure 2: Graph Structure of Notional Compound Encountered by UAS Supporting Law-Enforcement Operations

distance between nodes. The UAS's prior mean functions are set equal to their respective grand means, and RBF kernels with a bandwidth of 1 are the covariance functions. The UAS attempts to gain as much utility as possible and, rather than incur additional detection risk via exploration, will bed down in a final location to await the SWAT intervention. Assuming the UAS begins at Node 31, we explore the performance of each policy in this situation.

Building off results from Section 5.1, the same baseline policy parameter settings are used by the UAS. Table 4 shows the performance of each baseline. Whereas the size and geometry of the graph provided in Figure 2 complicate the identification of an optimal clairvoyant walk, preventing the identification of a policy's optimality gap, the myopic policy may still be used as a benchmark. The baseline UCB policy provides no improvement to this benchmark; it identifies the same walk as the myopic policy. But policies HP and SC improve over policy M, by differing amounts. Policy HP showed relatively minor improvement, but the improvement of policy SC was more significant. Such results exhibit clear qualitative behaviors in each policy's walk as well. Policy M and UCB never enter the south building, but did extensive exploration of the northwest building. Policy HP visited all three buildings, but only peered inside without substantive exploration. Policy SC visited all three buildings and conducted extensive surveillance of the south building, a beneficial choice given its relatively high density of larger rewards. All baseline policies neglected the northeast building where rewards are more sparse.

Note the contrasting performance of policy HP in Tables and 3 and 4. It shows that a policy's success can vary and the need for hyperparameter tuning. The baseline policy

Table 4: Performance of Baseline Policies in UAS Case Study

| Policy (π) | Parameter Setting(s) | Sequence of States Visited | Total Contribution Earned | Improvement over Myopic Policy |
|----------------|-------------------------|-------------------------------|------------------------------|-----------------------------------|
| M | - | 31-11-8-7-6-9-10 | 126.66 | - |
| UCB | $\lambda = 1$ | 31-11-8-7-6-9-10 | 126.66 | 0% |
| HP | $\alpha = 1; H = 3$ | 31-11-22-8 | 129.15 | 1.96% |
| SC | $\beta = 1$ | 31-11-8-22-26-27-28-29-30 | 173.29 | 36.81% |

HP substantially improved over policy M in Section 5.1, but provided no improvement when routing the UAS. Therefore, to explore the effect of hyperparameter tuning on policy performance, we consider the effects of parameterizing policy UCB with $\lambda \in \{1, 10\}$, policy HP with $(\alpha, H) \in \{0, 1, 10\} \times \{3, 4, 5\}$, and policy SC with $\beta \in \{1, 10, 100\}$. The performance of these policies, along with their corresponding walks, are provided in Table 5.

Table 5: Performance of Alternatively Parameterized Policies in UAS Case Study

| | Parameter | Sequence of | Total Contribution | Improvement over |
|----------------|----------------------|---|--------------------|------------------|
| Policy (π) | Setting(s) | Nodes Visited | Earned | Myopic Policy |
| \overline{M} | - | 31-11-8-7-6-9-10 | 126.66 | - |
| UCB^* | $\lambda = 1$ | 31-11-8-7-6-9-10 | 126.66 | 0% |
| UCB^{**} | $\lambda = 10$ | 31-11-8-22-26-27-28-23 | 161.73 | 27.69% |
| HP^* | $\alpha = 0; H = 3$ | 31-11-22-8 | 129.15 | 1.96% |
| HP^{**} | $\alpha = 0; H = 4$ | 31-11-31-8-22 | 135.83 | 7.24% |
| HP | $\alpha = 0; H = 5$ | 31-11-22-11-12 | 42.40 | -66.53% |
| HP | $\alpha = 1; H = 3$ | 31-11-22-8 | 129.15 | 1.96% |
| HP | $\alpha = 1; H = 4$ | 31-11-31-8-22 | 135.83 | 7.24% |
| HP | $\alpha = 1; H = 5$ | 31-11-22-11-12 | 42.40 | -66.53% |
| HP | $\alpha = 10; H = 3$ | 31-11-22-8-11 | 89.15 | -37.51% |
| HP | $\alpha = 10; H = 4$ | 31-11-31-8-22 | 135.83 | 7.24% |
| HP | $\alpha = 10; H = 5$ | 31 11 22 11 12 | 42.40 | -66.53% |
| SC^* | $\beta = 1$ | 31-11-8-22-26-27-28-29-30 | 173.29 | 36.81% |
| SC | $\beta = 10$ | 31 - 22 - 23 - 28 - 27 - 26 - 22 - 11 - 8 - 7 | 152.60 | 20.48% |
| SC^{**} | $\beta = 100$ | 31-22-23-28-27-26-25-24-21-22-11-8-7 | 207.88 | 64.12% |

^{*}Baseline parameter settings for each policy

These results show that the performances of policies UCB, HP, and SC were improved by exploring alternative hyperparameter options. Improvement over policy M was largest for policies UCB and SC with gains of approximately 27% and 28%, respectively. Policy HP improved as well. The substantive gains made by the tuned policy UCB result from its exploration of the south building. The first seven nodes in its walk coincide with those of the baseline policy HP. This increased exploration makes

^{**}Best performing parameter settings for each policy

sense given its larger value of λ . Alternatively, the tuned policy HP chose a walk that more thoroughly explored both the south and northwest buildings. This behavior was driven by a larger β ; which makes sense since increased β -values favor a longer search for each subproblem. However, based on the randomness of Algorithm 2, a larger β does not guarantee improved performance—note the performance of policy SC with $\beta=10$ in Table 5.

The behavior of policy HP is more nuanced. Multiple parameter choices yield walks of similar quality. Across every level of α , the policy with H=4 performed best and identified the same walk. Similarly, whenever H=5, policy HP substantively underperformed policy M. Thus, for this example, there is little benefit from varying the exploration parameter, α ; and by increasing H to forecast too far ahead, the traveler's performance was degraded. This outcome raises questions regarding how the specifics of a problem instance affects policy performance, a topic we explore in the next section.

5.3. Policy Performance on Random Networks

This section studies different network structures to determine how they affect the policies' decisions. We generate many random networks and evaluate each policy over them. For each network, we use the same features for the node rewards and edges, and the same true reward and cost functions, as in Section 5.1. The nodes for each instance are randomly placed on coordinates of P, the prior mean functions are defined as their respective grand means, and RBF kernels with bandwidth one are used as covariance functions. True node rewards and edge costs are also calculated as in Section 5.1 based upon the random graph structure and node locations.

We generate random networks from the Erdös–Rényi model. Erdös–Rényi models have two parameters: the number of nodes $|\mathcal{N}|$ and the edge creation probability p [26]. For a range of $|\mathcal{N}|$ and p values, we generate networks, discarding graphs that are not connected. We also ensure that each node has a self-loop, so that the exploration can terminate. Table 6 shows values $|\mathcal{N}|$ and p that we explored. Thirty connected graphs for each $|\mathcal{N}|$ and p combination were generated and analyzed.

Across each of the Erdös–Rényi settings, we examine the performance of the policy parameter settings explored in Section 5.2. Table 6 shows the factor levels used for each of policy UCB, HP, and SC. These levels provide distinct incentives for each policy. For example, by increasing H in policy HP, the traveler has additional forethought; increasing λ in policy UCB means the traveler explores more. Our goal is to identify how well a policy parameterization generalizes across similar problems.

Table 7 summarizes our experiment, indicating the best-performing policy parameters as well as statistical summaries of their performance over 30 draws from each Erdös–Rényi setting. Columns one and two specify the nine Erdös–Rényi parameter combinations. Columns three to six identify the best settings for the UCB, HP, and SC policies. Columns seven through nine report the 95% confidence intervals on the average improvement over the myopic policy, giving us a metric for algorithmic effectiveness. Policy M is used as a baseline instead of the clairvoyant's solution, which becomes intractable as the graph grows in complexity.

Table 6: Parameter Values

| Parameter | Settings | | |
|-----------------|-------------------|--|--|
| $ \mathcal{N} $ | {20, 50, 80} | | |
| p | $\{0.2,0.5,0.8\}$ | | |
| λ | $\{0^*, 1, 10\}$ | | |
| H | $\{3,4,5\}$ | | |
| α | $\{0, 1, 10\}$ | | |
| β | $\{1, 10, 100\}$ | | |

^{*}Represents myopic policy

Table 7: Experimental Design Results

| Erdös–Rényi | | Bes | Best Algorithmic | | | Improvement Over | | |
|--------------------|-----|------|--------------------|----------|-----|---|---------------|--|
| Parameter Settings | | Para | Parameter Settings | | | Myopic Policy (%) | | |
| $ \mathcal{N} $ | p | λ | H | α | β | UCB HP | SC | |
| 20 | 0.2 | -10 | 4 | 0 | 1 | $20.31 \pm 0.32 16.34 \pm 0.12 33.$ | 08 ± 0.13 | |
| 20 | 0.5 | -1 | 5 | -10 | 100 | 1.54 ± 0.14 23.51 ± 0.21 $20.$ | 81 ± 0.26 | |
| 20 | 0.8 | -10 | 3 | -1 | 1 | 13.59 ± 0.25 31.29 ± 0.28 $70.$ | 20 ± 0.41 | |
| 50 | 0.2 | -10 | 5 | -10 | 100 | 16.72 ± 0.47 40.53 ± 0.52 29. | 38 ± 1.44 | |
| 50 | 0.5 | -10 | 3 | -1 | 10 | $3.43 \pm 1.11 27.37 \pm 0.98 27.$ | 58 ± 1.38 | |
| 50 | 0.8 | -1 | 4 | -10 | 100 | -17.36 ± 0.92 27.16 ± 0.66 38. | 61 ± 1.28 | |
| 80 | 0.2 | -1 | 5 | -10 | 10 | 27.28 ± 1.33 53.38 ± 0.93 $22.$ | 93 ± 2.06 | |
| 80 | 0.5 | -1 | 5 | -1 | 100 | -3.47 ± 1.18 26.63 ± 1.57 $32.$ | 52 ± 2.01 | |
| 80 | 0.8 | -10 | 5 | -10 | 10 | -5.29 ± 0.68 19.43 ± 1.73 99. | 56 ± 2.48 | |

Table 7 shows that policy UCB does not always improve over policy M. The increased exploration generally pays off for simpler networks but not for complex ones. Policies HP and SC consistently outperform the myopic policy for all nine problem cases, implying these are superior choices for the types of networks we study. As in Section 5.1, the improvement is often dramatic. Policy HP's minimum average improvement was 16% and its maximum was 54%. Policy SC's average improvement ranged from 20% to nearly 100%.

Interpreting the relationship between network size and sparsity on policy success is difficult. For $|\mathcal{N}|=20$, policy HP's expected performance over policy M increases as the graphs become more dense, whereas for $|\mathcal{N}|=80$, the opposite occurs. Policy SC attains its best performances for the densest graphs examined in our experiments, with average improvement over M most pronounced for $|\mathcal{N}|=20,80$, likely due to its ability to consider cycles. Finally, in contrast to policy UCB, policy HP tends to benefit from exploration; in all but one Erdös–Rényi setting, $\alpha>0$ was preferred. A larger β often benefited policy SC, but the randomness of its search meant that, in some settings, smaller β -values found better solutions.

Although policy HP and SC are globally preferable to policy UCB, no single policy dominates. The most effective policy depends upon the specific Erdös–Rényi parameters. The improvements over the myopic policy reinforce this finding, and the confidence intervals quantify the variability in the outcomes. Moreover, there are no universally best policy parameter settings for all situations. Instead, parameter adjustments are necessary to optimize each policy, dependent on the unique conditions of each problem type. Nonetheless, significant improvement over policy M is achievable given the correct implementation of either policy HP or policy SC. This insight highlights the importance of an informed, context-sensitive approach to policy selection for each application. It also suggests that the increased complexity in the subproblems generated by policies HP and SC can yield substantial dividends, justifying the increased computational effort.

6. Conclusion

We study movement of a traveler along a graph in which a random reward is gained upon the first visit to a node and a random cost is incurred for each edge traversal. The traveler knows the graph's adjacency matrix and his starting position. The Bayesian traveler has Gaussian process priors about the rewards and costs, leading to a sequential decision-making problem that applies to many other situations than just graph traversal (e.g., changing jobs, selecting college courses, investment in security, convoy routing in hostile territory, portfolio management).

The problem is NP-hard, and so one needs heuristic policies to find a solution. We compared four policies that balance exploration and exploitation in different ways to heuristically optimize expected utility. The performance of these policies was examined on a small network and on random (connected) graphs from an Erdös–Rényi model whose parameters were varied in an experimental design.

Additional theoretical extensions exist. For example, one may consider how the accuracy of the traveler's beliefs interacts with the policy type and network structure.

It may be the case that some policies perform better when the traveler's priors are initially accurate (inaccurate) or when the network is dense (sparse). Such issues also drive extensions of this work that consider value-function approximation policies. The efficacy of pre-training such policies is affected by the accuracy of the traveler's beliefs, and future work may consider when such beliefs are accurate enough to warrant the additional computational burden. Moreover, in future studies, one could model the costs and rewards jointly, modify the formulation such to consider noisy costs and rewards, or propose an adversarial framework in which an opponent can perturb edge costs or node rewards. Adaptations of policies provided in other work [e.g., see 6, 40] or applications to relevant scenarios in the literature [e.g., see 37, 9, 23] may also be possible given their relationship to the Bayesian graph traversal problem. Finally, given that none of our policies dominates the others, future research could study alternative policies which balance solution quality against computational effort, or identify the network characteristics that should guide policy choice.

Acknowledgments

This work was supported by the Office of Naval Research Grant 6000012277 GRA as well as by Air Force Office of Scientific Research grant 21RT0867.

Disclaimer

The views expressed in this article are those of the authors and do not reflect the official policy or position of the United States Air Force, United States Department of Defense, or United States Government.

References

- [1] Vural Aksakalli, O Furkan Sahin, and Ibrahim Ari. An AO* Based Exact Algorithm for the Canadian Traveler Problem. *INFORMS Journal on Computing*, 28(1): 96–111, 2016.
- [2] Lina Al-Kanj, Warren B Powell, and Belgacem Bouzaiene-Ayari. The information-collecting vehicle routing problem: Stochastic optimization for emergency storm response. arXiv preprint arXiv:2301.06497, 2023.
- [3] OP Bagai. The Distribution of the Generalized Variance. The Annals of Mathematical Statistics, 36(1):120–130, 1965.
- [4] Russell W Bent and Pascal Van Hentenryck. Scenario-based planning for partially dynamic vehicle routing with stochastic customers. *Operations Research*, 52(6): 977–987, 2004.
- [5] Juan S. Borrero, Oleg A. Prokopyev, and Denis Sauré. Sequential Shortest Path Interdiction with Incomplete Information. *Decision Analysis*, 13(1):68–98, 2016.

- [6] David B Brown and James E Smith. Optimal sequential exploration: Bandits, clairvoyants, and wildcats. *Operations research*, 61(3):644–665, 2013.
- [7] Martin Dietrich Buhmann. Radial basis functions. Acta Numerica, 9:1–38, 2000.
- [8] Alon Cohen, Yonathan Efroni, Yishay Mansour, and Aviv Rosenberg. Minimax Regret for Stochastic Shortest Path. In M. Ranzato, A. Beygelzimer, Y. Dauphin, P. S. Liang, and J. Wortman Vaughan, editors, Advances in Neural Information Processing Systems, volume 34, pages 28350–28361. Curran Associates, Inc., 2021.
- [9] Trygve Olav Fossum, Cédric Travelletti, Jo Eidsvik, David Ginsbourger, and Kanna Rajan. Learning excursion sets of vector-valued gaussian random fields for autonomous ocean sampling. *The annals of applied statistics*, 15(2):597–618, 2021.
- [10] Peter Frazier, Warren Powell, and Savas Dayanik. The Knowledge-Gradient Policy for Correlated Normal Beliefs. *INFORMS Journal on Computing*, 21(4):599–613, 2009.
- [11] Peter I. Frazier. Bayesian Optimization. In *INFORMS TutORials in Operations Research: Recent Advances in Optimization and Modeling of Contemporary Problems*, pages 255–278. INFORMS, 2018.
- [12] Peter I. Frazier. A Tutorial on Bayesian Optimization. arXiv preprint arXiv:1807.02811, 2018.
- [13] Jacob R Gardner, Matt J Kusner, Zhixiang Eddie Xu, Kilian Q Weinberger, and John P Cunningham. Bayesian optimization with inequality constraints. In *ICML*, volume 2014, pages 937–945, 2014.
- [14] Roman Garnett. *Bayesian Optimization*. Cambridge University Press, Cambridge, UK, 2023.
- [15] Jinil Han, Chungmok Lee, and Sungsoo Park. A Robust Scenario Approach for the Vehicle Routing Problem with Uncertain Travel Times. *Transportation Science*, 48 (3):373–390, 2014.
- [16] Joseph Douglas Horton. A Polynomial-Time Algorithm to Find the Shortest Cycle Basis of a Graph. SIAM Journal on Computing, 16(2):358–366, 1987.
- [17] Stefan Hougardy, Fabian Zaiser, and Xianghui Zhong. The approximation ratio of the 2-Opt Heuristic for the metric Traveling Salesman Problem. *Operations Research Letters*, 48(4):401–404, 2020.
- [18] International Association of Chiefs of Police. Small Unmanned Aircraft Systems. https://www.theiacp.org/sites/default/files/2020-06/Unmanned% 20Aircraft%20FULL%20-%2006222020.pdf, 2020.

- [19] International Association of Fire Chiefs. UAS Tactics. https://www.iafc.org/topics-and-tools/communications-technology/uas-toolkit/uas-resource/uas-tactics, 2024.
- [20] David Karger, Rajeev Motwani, and Gurumurthy DS Ramkumar. On approximating the longest path in a graph. *Algorithmica*, 18(1):82–98, 1997.
- [21] Tomás Lagos, Ramón Auad, and Felipe Lagos. The online shortest path problem: Learning travel times using a multiarmed bandit framework. *Transportation Science*, 2024.
- [22] Churlzu Lim, J Neil Bearden, and J Cole Smith. Sequential Search with Multiattribute Options. *Decision Analysis*, 3(1):3–15, 2006.
- [23] Seth McCammon and Geoffrey A Hollinger. Topological path planning for autonomous information gathering. *Autonomous Robots*, 45(6):821–842, 2021.
- [24] Yifei Min, Jiafan He, Tianhao Wang, and Quanquan Gu. Learning Stochastic Shortest Path with Linear Function Approximation. In Kamalika Chaudhuri, Stefanie Jegelka, Le Song, Csaba Szepesvari, Gang Niu, and Sivan Sabato, editors, Proceedings of the 39th International Conference on Machine Learning, volume 162 of Proceedings of Machine Learning Research, pages 15584–15629. PMLR, 17–23 Jul 2022.
- [25] National Urban Security Technology Laboratory. Blue Unmanned Aircraft Systems for First Responders. https://www.dhs.gov/sites/default/files/2024-03/24_03_1_st_blueuasfocusgroupreport.pdf, 2024.
- [26] Mark Newman. Networks. Oxford University Press, Oxford, UK, 2nd edition, 2018.
- [27] Evdokia Nikolova and David R. Karger. Route Planning under Uncertainty: The Canadian Traveller Problem. In Proceedings of the Twenty-Third AAAI Conference on Artificial Intelligence, pages 969–974, Cambridge, MA, USA, 2008. Association for the Advancement of Artificial Intelligence, AAAI Press.
- [28] Warren B Powell. A unified framework for stochastic optimization. European Journal of Operational Research, 275(3):795–821, 2019.
- [29] Warren B. Powell. Reinforcement Learning and Stochastic Optimization: A Unified Framework for Sequential Decisions. John Wiley & Sons, Inc., Hoboken, NJ, USA, 2022.
- [30] Warren B Powell, Patrick Jaillet, and Amedeo Odoni. Stochastic and dynamic networks and routing. *Handbooks in operations research and management science*, 8:141–295, 1995.
- [31] Ilya O Ryzhov and Warren B Powell. Information Collection on a Graph. *Operations Research*, 59(1):188–201, 2011.

- [32] Ilya O Ryzhov and Warren B Powell. Information Collection for Linear Programs with Uncertain Objective Coefficients. SIAM Journal on Optimization, 22(4): 1344–1368, 2012.
- [33] Nicola Secomandi. A rollout policy for the vehicle routing problem with stochastic demands. *Operations Research*, 49(5):796–802, 2001.
- [34] Bobak Shahriari, Kevin Swersky, Ziyu Wang, Ryan P. Adams, and Nando de Freitas. Taking the Human Out of the Loop: A Review of Bayesian Optimization. *Proceedings of the IEEE*, 104(1):148–175, 2016.
- [35] Davood Shiri and F Sibel Salman. On the randomized online strategies for the k-Canadian traveler problem. *Journal of Combinatorial Optimization*, 38(1):254–267, 2019.
- [36] Ninja Soeffker, Marlin W Ulmer, and Dirk C Mattfeld. Stochastic dynamic vehicle routing in the light of prescriptive analytics: A review. *European Journal of Operational Research*, 298(3):801–820, 2022.
- [37] Junghun Suh, Joonsig Gong, and Songhwai Oh. Fast sampling-based cost-aware path planning with nonmyopic extensions using cross entropy. *IEEE Transactions on Robotics*, 33(6):1313–1326, 2017.
- [38] Gary J. Summers. Friction and Decision Rules in Portfolio Decision Analysis. Decision Analysis, 18(2):101–120, 2021.
- [39] Hamdy A Taha. Operations research: an introduction. Pearson Education India, 2013.
- [40] Lawrence Thul and Warren B Powell. An information-collecting drone management problem for wildfire mitigation. arXiv preprint arXiv:2301.07013, 2023.
- [41] Chenhao Zhang, Jason D Hartline, and Christos Dimoulas. Karp: a language for np reductions. In *Proceedings of the 43rd ACM SIGPLAN International Conference on Programming Language Design and Implementation*, pages 762–776, 2022.